PROGRESS TOWARD A HIGGS FACTORY

B. Freemire
Illinois Institute of Technology
for the Muon Accelerator Program

Bright muon sources offer the potential to study neutrinos, the Higgs boson, and search for new physics at the energy frontier. The Muon Accelerator Program (MAP) in the United States began in 2010, with the goal of proving the feasibility of building such a machine. MAP's efforts are nearing completion, and a great deal of progress has been made on each of the accelerator's subsystems. A Higgs factory allows for s-channel production of the Higgs, amounting to ∼13,500 Higgs produced per 10^7 seconds, while providing a beam energy spread on the order of 0.004% with which to measure the Higgs width. A Higgs factory relies on a high power proton driver and suitable target, significant six dimensional cooling, and moderate reacceleration.

1 Introduction

A muon collider would offer an exceptional tool with which to study the Higgs boson. Similar to the case of the W and Z bosons, a precision machine may be desirable and necessary to study the Higgs boson in detail to compliment the results from the LHC. A direct measurement of the cross section is enhanced in a muon collider as opposed to an electron-positron collider, due to the s-channel coupling to a scalar being proportional to lepton mass. The s-state production offers a clean signal that would allow the narrow width and most decay channels to be measured with great accuracy. Figure 1 shows the expected signal and background for two decay channels, utilizing the 0.003% energy resolution possible due to significantly less beamstrahlung than an e^+e^- collider.

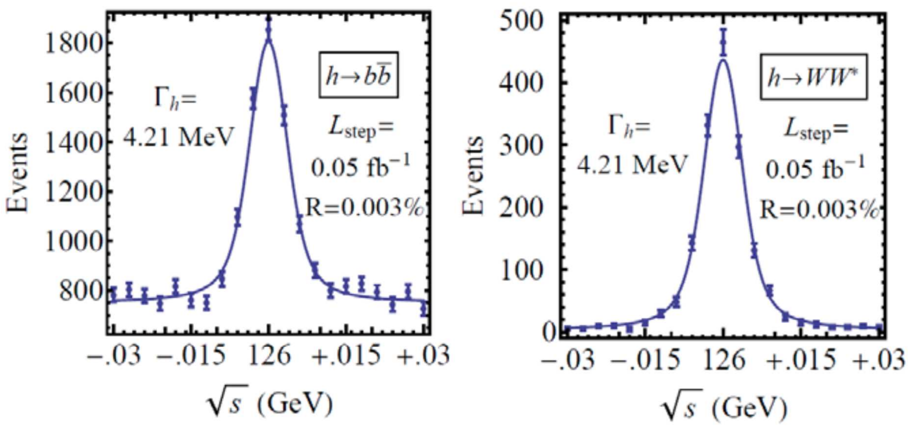

Figure 1 – Number of events of the Higgs signal plus backgrounds and statistical errors for $h \to b\bar{b}$ (left) and $h \to WW^*$ (right) [3]. Both assume an integrated luminosity of 1 fb^{-1} and energy resolution of 0.003%.

The footprint of a Muon Collider is an order of magnitude smaller than either a pp or e^+e^- collider due to the elementary nature of the electron, and the ability to accelerate in rings. Figure 2 shows the footprint of a Muon Collider, the LHC, and estimates of the ILC, CLIC, and VLHC overlaid on Chicago for reference.

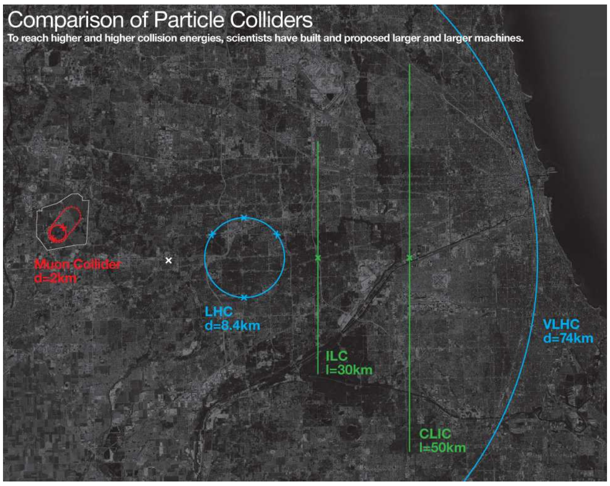

Figure 2 – Current (LHC) and possible future colliders (Muon Collider, ILC, CLIC, VLHC) laid over the Chicago area [1].

2 Higgs Factory Based on a Muon Collider

A Higgs Factory based on a Muon Collider has the additional advantage of easily accommodating a Neutrino Factory on the same site because of the overlap of many required subsystems. Figure 3 shows the subsystems for both a Neutrino Factory and Muon Collider. The expected performance and design parameters for a Higgs Factory are listed in Table 1.

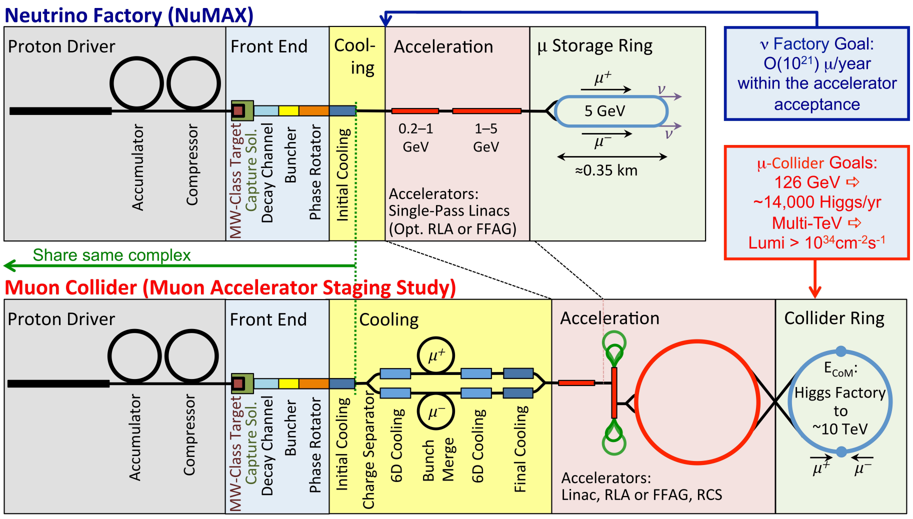

Figure 3 – Cartoon showing the systems for a Neutrino Factory (top) and Muon Collider (bottom) [2]. Note the two machines share the same complex from the proton driver to the initial cooling.

3 Higgs Factory Subsystems

The following sections will be devoted to summarizing the current progress on the major subsystems of a Muon Collider as they apply to a Higgs Factory.

Table 1: Muon Collider baseline parameters [2].

Parameter	Units	Higgs Factory Value	3 TeV Value
CoM Energy	TeV	0.126	3.0
Avg. Luminosity	10^{34} cm^{-2}s^{-1}	0.008	4.4
Beam Energy Spread	%	0.004	0.1
Higgs/10^7 sec		13,500	200,000
Circumference	km	0.3	4.5
No. of IPs		1	2
Repetition Rate	Hz	15	12
$\beta*$	cm	1.7	0.5 (0.3-3)
No. muons/bunch	10^{12}	4	2
No. bunches/beam		1	1
Norm. Trans. Emittance, ϵ_{TN}	π mm-rad	0.2	0.025
Norm. Long. Emittance, ϵ_{LN}	π mm-rad	1.5	70
Bunch length, σ_s	cm	6.3	0.5
Beam Size @ IP	μm	75	3
Beam-beam parameter / IP		0.02	0.09
Proton Driver Power	MW	4	4
Wall Plug Power	MW	200	230

3.1 Front End

Figure 4 shows a cartoon of the front end of a Muon Collider, including the the target, chicane, drift and absorber, buncher, phase rotator, and initial cooling, as well as an illustration of the longitudinal phase space of the beam through the drift, bunch, and phase rotation.

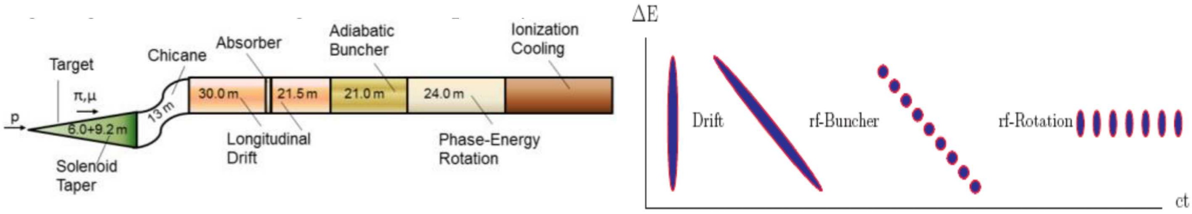

Figure 4 – Cartoon showing the subsystems of the front end of a muon accelerator (left) [4] and beam bunching and phase rotation (right) [5].

The baseline for a Higgs Factory relies on a 1-4 MW proton driver and a target station capable of handling such a powerful beam. A cartoon of the target station is shown in Fig. 5. Two target materials are under consideration: solid graphite [6], and liquid mercury [7]. A 20 T solenoid field is utilized to capture pions, tapering to 2 T at the end of the capture system. Because of the extreme radiation environment of the target, an inner 5 T resistive coil insert is used in conjunction with an outer 15 T superconducting solenoid to provide the necessary 20 T. Shielding is provided for the superconducting coils in the form of tungsten beads cooled with helium gas. Optimization of the target design has been performed, with yields of about 0.022 muons/proton/GeV in the 40-180 MeV range for graphite, and about 10% larger for liquid mercury in a 15 T magnetic field [8]. Increasing the magnetic field or acceptance energy increases the yield for both targets significantly (up to about 0.05 muons/proton/GeV for liquid mercury with a 15$\rightarrow$4 T taper and 40-300 MeV kinetic energy range).

To select out high energy particles and protons, a chicane and absorber are utilized (see Fig. 6) [9]. Particles above 800 MeV/c are lost in the chicane, while lower momentum protons are mostly removed by a 10 cm absorber place 30 m downstream of the chicane. Power deposition

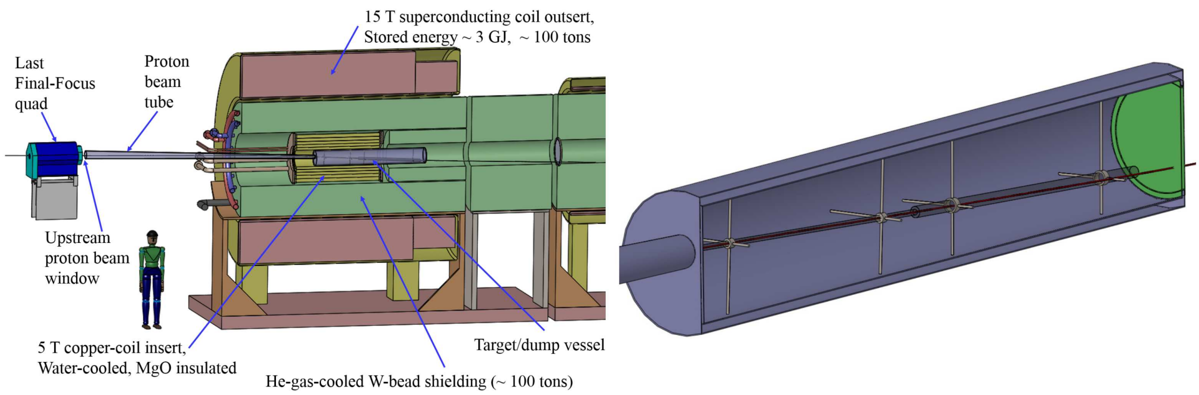

Figure 5 – Cartoon showing the target station (left) and target vessel for the case of a graphite target (right) [6].

in the superconducting coils in the chicane is an issue, and shielding must be sufficient to ensure the power density deposited is below the superconducting operational limit (see Fig. 6).

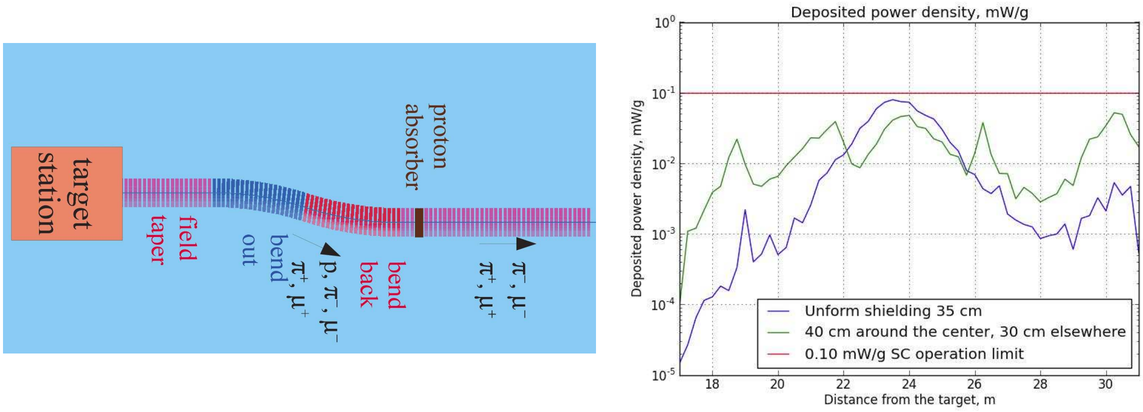

Figure 6 – Cartoon of the chicane and proton absorber (left), and simulated deposited power density in the chicane (right) [9]. The power density must be kept below the 0.10 mW/g superconducting operational limit.

The buncher and phase rotator consist of a series of RF cavities to bunch the beam and decelerate higher energy muons and accelerate lower energy muons [10]. The bunching system utilizes 56 normal conducting RF cavities with frequencies tapering from 494 to 370 MHz and gradients up to 14.3 MV/m over 21 m. The phase rotator utilizes cavities further tapering to 325 MHz over 24 m, with a constant gradient of 20 MV/m. A matching section is then used to lead into the cooling channel. Figure 7 shows the longitudinal phase space at the end of the phase rotator and muon yield leading into the cooling channel.

3.2 Cooling

Muons collected from colliding a high power proton beam with a target have a phase space much too large to produce the luminosity needed for a Higgs Factory or multi-TeV collider. As such, many orders of magnitude cooling is required. The progression of the transverse and longitudinal emittances of the beam is shown in Fig. 8, where it can be seen the small longitundinal emittance leads to the exquisite energy resolution mentioned above.

Muon beams of both signs are cooled via ionization cooling [11, 12]. The Muon Ionization Cooling Experiment is currently running at Rutherford Appleton Laboratory with the purpose of demonstrating the feasibility of building a ionization cooling cell [13–15].

Ionization cooling intrinsically works transversely, so to perform the 6D cooling required to attain the emittances in Fig. 8, emittance exchange must be utilized. There are two schemes to

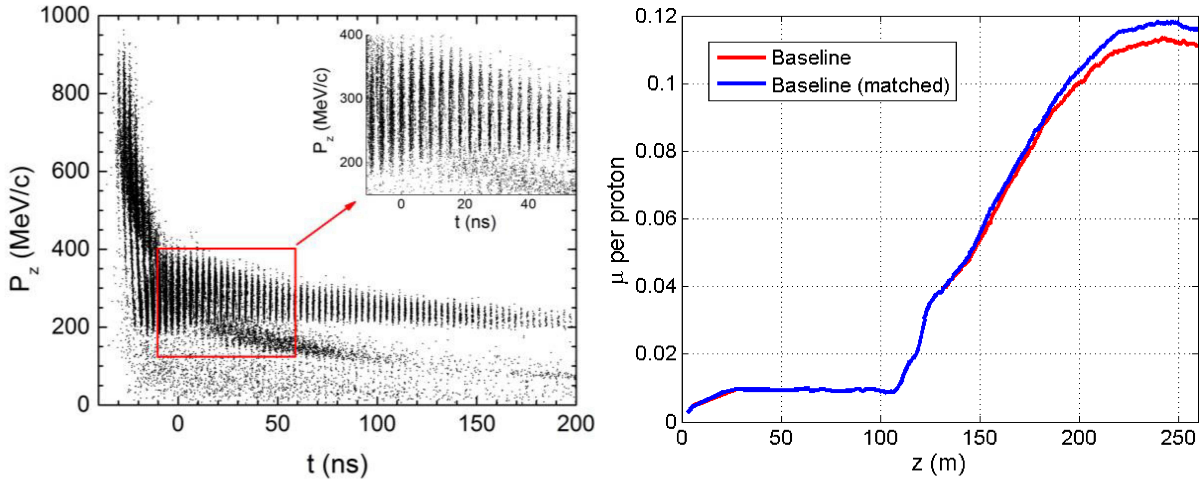

Figure 7 – Longitudinal phase space distribution of the beam at the exit of the phase rotator (left), and optimized muon yield after the matching section before cooling (right) [10].

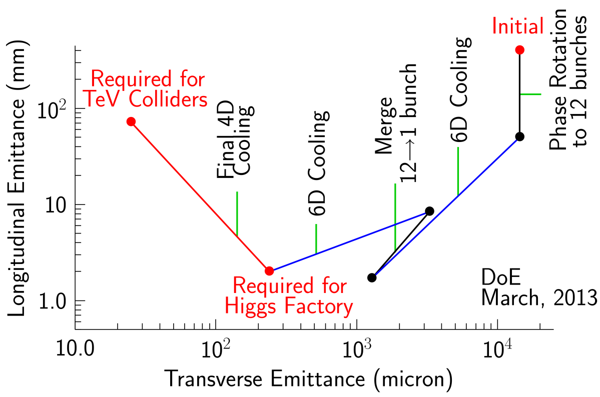

Figure 8 – Longitudinal versus transverse emittance plot showing the phase space manipulation of the beam from the initial distribution through requirements for a Higgs Factory and finally a TeV collider [2]. The current bunch scheme calls for 21 bunches, as opposed to the 12 detailed in this plot.

accomplish this, the Rectilinear and Helical Cooling Channels. The Rectilinear Cooling Channel (RCC) utilizes vacuum RF cavities, discrete wedge shaped absorbers, and tilted solenoids [16]. The Helical Cooling Channel (HCC) utilizes high pressure gas filled RF (HPRF) cavities, continuous gaseous absorber, and helical solenoids [17, 18]. Both schemes are shown pictorally in Fig. 9.

Both cooling channels provide a final 6D emittance close to the required Higgs Factory specification. Significant progress has been made in validating the technology for the two schemes. The difficulty in the Rectilinear design stems from RF breakdown in the presence of strong external magnetic fields, and in the Helical design from the complex magnet design, and incorporating RF cavities within the magnet bores.

3.3 Collider Ring

The layout of one half of a Higgs Factory collider lattice is shown in Fig. 10, along with the beam size in the interaction region. The challenges in the design stem from the large aperture superconducting magnets needed to provide a small beta function at the interaction point required to meet the luminosity specification, and the need to protect the superconducting coils from muon decay products. The design β^* is 2.5 cm, however it can be varied from 1.5 to 10 cm without perturbing the dispersion function by adjusting the gradients in the matching sections, and the momentum acceptance is greater than $\pm 5\%$ [20].

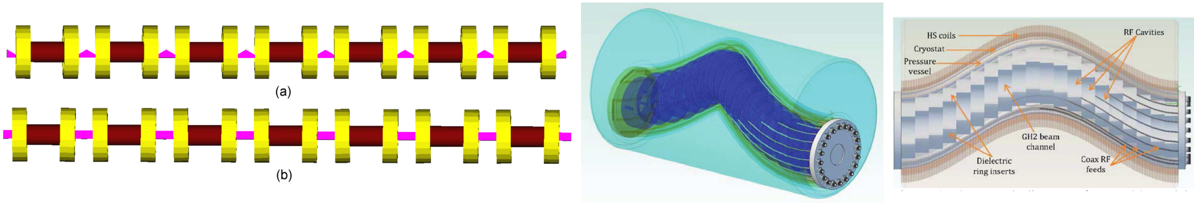

Figure 9 – Two 6D cooling channel schemes. The Rectilinear Channel, left, with top (a) and side (b) views, showing RF cavities (red), solenoid coils (yellow), and wedge absorbers (magenta) [16]. The Helical Channel, with a 3D cartoon of one cooling cell (center), and a cutaway view (right) [19].

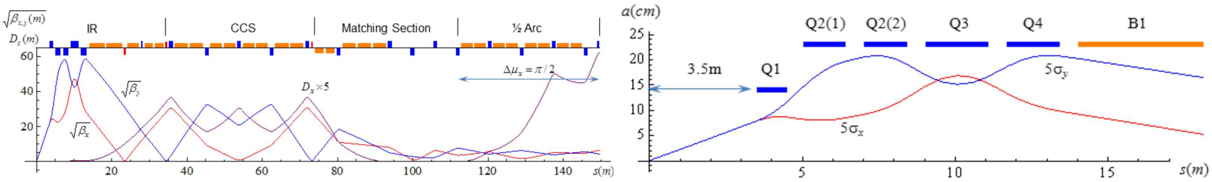

Figure 10 – Layout and optics functions for one half of the ring (left), and layout and beam size in the interaction region (right) [20].

4 Conclusion

A Muon Accelerator offers excellent physics results, allowing for both a Neutrino Factory and Muon Collider. In particular, a Muon Collider based Higgs Factory would provide excellent resolution on the Higgs resonance, with more precision than either the LHC or a similar electron-positron collider. The Muon Accelerator Program has made significant progress in demonstrating the technology required for the subsytems of a Higgs Factory, including the target, front end, cooling, and collider ring. The envisioned machine would provide $\sim$13,500 Higgs per 10^7 seconds, with a beam energy spread of 0.004%.

Acknowledgments

The work presented here has been supported by Fermi Research Alliance, LLC under contract No. DEAC0207CH11359.

References

1. Muon Accelerator Program website: http://map.fnal.gov.
2. J-P. Delahaye, *et al*, "Enabling Intensity and Energy Frontier Science with a Muon Accelerator Facility in the U.S.", FERMILAB-CONF-13-307-APC, 2013.
3. T. Han and Z. Liu, *Phys. Rev.* D **87**, 033007 (2013).
4. D. Stratakis and D.V. Neuffer, *J. Phys. G: Nucl. Part. Phys.* **41**, 125002 (2014).
5. D.V. Neuffer, "Muon Capture for the IDS Neutrino Factory," in *Proc. of PAC'09*, Vancouver, May 2009, TU1GRC05, p. 660.
6. K.T. McDonald *et al*, "Target System Concept for a Muon Collider/Neutrino Factory," in *Proc. of IPAC'14*, Dresden, June 2014, TUPRI008, p. 1568.
7. I. Efthymiopoulos *et al*, "The MERIT(nTOF-11) High Intensity Liquid Mercury Target Experiment at the CERN PS," in *Proc. of EPAC'08*, Genoa, June 2008, MOPC087, p. 262.
8. X. Ding *et al*, "Carbon and Mercury Target Systems for Muon Colliders and Neutrino Factories," in *Proc. of IPAC'16*, Busan, May 2016, TUPMY044, p. 1641.
9. P. Snopok *et al*, "Energy Deposition in Magnets and Shielding of the Target System of a Staged Neutrino Factory," in *Proc. of NAPAC'13*, Pasadena, Oct. 2013, THPMA10, p. 1376.

10. D. Stratakis *et al*, "Overview of a Muon Capture Section for Muon Accelerators," in *Proc. of IPAC'14*, Dresden, June 2014, TUPRI008, p. 1398.
11. G.I. Budker, "Accelerators and Colliding Beams," in *Proc. of 7th International Conference on High-energy Accelerators*, HEACC 1969, C690827, p. 33-39.
12. Y.M. Ado and V.I. Balbekov, *Atomnaya Energiya* **31**, No. 1, p. 40-44, 1971.
13. F. Drielsma *et al*, "Measurement of Emittance in the Muon Ionization Cooling Experiment," *These Proceedings*, Quy Nhon, Aug. 2016.
14. R. Bayes *et al*, "Measurements of the Multiple Coulomb Scattering of Muons by MICE," *These Proceedings*, Quy Nhon, Aug. 2016.
15. Y. Karadzhov *et al*, "Ionization Cooling Demonstration," *These Proceedings*, Quy Nhon, Aug. 2016.
16. D. Stratakis and R.B. Palmer, *Phys. Rev. ST Accel. and Beams* **18**, 031003 (2015).
17. Y. Derbenev and R.P. Johnson, *Phys. Rev. ST Accel. and Beams* **8**, 041002 (2005).
18. K. Yonehara *et al*, "Muon Beam Emittance Evolution in the Helical Ionization Cooling Channel for Bright Muon Sources," in *Proc. of IPAC'15*, Richmond, May 2015, TUPTY074, p. 2203.
19. R.P. Johnson *et al.*, "Muon Beam Helical Cooling Channel Design," in *Proc. COOL'13*, Murren, June 2013, MOAM2HA03, p. 21.
20. A.V. Zlobin *et al*, "Preliminary Design of a Higgs Factory $\mu^+\mu^-$ Storage Ring," in *Proc. of IPAC'13*, Shanghai, May 2013, TUPFI061, p. 1487.